An initial characterisation of a tidal stream turbine on a drive train test rig

Edith Rojo-Zazueta, Matthew Allmark, Paul Prickett, Roger Grosvenor

Abstract—**The potential of tidal stream turbines simulations on steady-state conditions by the use of a drive train test rig is considered. An initial assessment of two case scenarios is developed to furtherly assess the availability of replicating a theoretical model to the experimental model. It has been demonstrated that a drive train test rig is able to represent power curves of a 0.5 m diameter turbine with velocities from 0.5 to 1.8 ms^{-1} given its torque value and its rotational frequency. IndraWorks Engineering is being used to obtain the rotor and generator signals and review the losses through a horizontal axis tidal turbine drivetrain. This provides a first order approximation for the use of the test rig with non-steady state conditions and develop condition monitoring techniques.**

Keywords—**Condition-based maintenance, tidal stream turbine, generator test rig.**

I. Introduction

The tidal stream energy sector is still in its infancy and it must overcome several technological barriers to prove the reliability and affordability of its devices. Magagna and Uilhlein [1] have found that, within the four main bottlenecks that have slowed down the development of Horizontal Axis Tidal Turbines (HATTs), the most important issue to address is the lack of long-term reliability due to the harsh environment turbines operate within. Consequently, this leads to financial issues which promote investor uncertainty. Without addressing this issue developers are unable to take the technology readiness level (TRL) to forward to the next stage. Currently, HATTs are said to be limited to a TRL of 7-8 [2] and any advancement is constrained by the lack of funding and an associated high levelised cost of energy (LCoE). This does not suggest that the sector is yet in position to move to a full commercial-scale stage. Much of the research reported has accomplished a TRL of 4, which means that design validation and intermediate testing at scale (e.g. flume test scale of 1:10) has been achieved.

The authors gratefully acknowledge CONACYT Mexico for the financial support given for this project.

The authors E. Rojo-Zazueta, M. Allmark, P. Prickett and R. Grosvenor are with the Cardiff Marine Energy Research Group (CMERG) located in the School of Engineering at Cardiff University, Cardiff South Glamorgan, CF24 3AA Wales, UK. Their e-mails are: RojoZazuetaEG@cardiff.ac.uk, AllmarkMJ1@cardiff.ac.uk, Prickett@cardiff.ac.uk and Grosvenor@cardiff.ac.uk.

The approach taken to date has largely focused on optimising HATT performance using computational fluid dynamics (CFD) modelling. These models are then compared with results acquired via experimental testing, using for example flume tanks, to validate them. CFD is an important and very valuable research tool but can be time consuming and potentially expensive. There are a small number of projects that have been able to advance to a TRL of 7-8. One example is Atlantis Resources being deployed in the Pentland Firth. Work has finished on the construction phase of what may be considered to be the world's largest tidal stream turbine array [3]. However, according to some assessments this may still be defined as a small scale project since it is under 20 GW generation [1]. The nature of the challenges to be met suggest that there is still great potential in meeting them by identifying other possible solutions.

In order to underpin the long-term reliability of HATTs, their components' operating constraints, device maintenance and the operational costs are of particular concern. One of the most utilised tools in industries with similar levels of plant complexity is condition-based maintenance (CBM). This is an asset management technique that uses the regular assessment of the actual operating and health condition of a component or system to optimise its total operation [4]. CBM indicates when maintenance should be performed based on signs of decreasing performance or possible failure. Some advantages of introducing CBM to the HATT industry would be to improve device reliability, reduce maintenance costs and improve the competitiveness of HATTs against other renewable energy technologies. However, implementing CBM requires the associated development of condition monitoring (CM) techniques to provide the information needed to underpin the approach. This consideration produces the need for an effective vehicle that can be used for testing CM approaches. Engineering CM elements that can be used to predict possible failures under real conditions would be very costly. One reason for this is the need to consider how the HATT operation can be affected by specific faults. Often analysing this means that damaged components need to be installed to verify if the associated failure is being correctly detected. The need and associated cost of this has not been fully considered within the sector.

Even though that CM techniques for HATTs research is very limited, there has been some work reported [5-8]. In general these have explored the application of signal

processing based on frequency analysis of a particular HATT drive train component. Focusing on the previous research undertaken by the Cardiff Marine Energy Group (CMERG), the use of a drive train simulator test bed at 1/20th scale has been developed to create representative HATT simulations [9]. This has been utilised to engineer CM algorithms to develop and test monitoring approaches under steady-state and non-steady-state conditions. The main advantage of utilising this test rig is its ability to adapt to a variety of operating conditions for real time HATT simulations, and hence enable the testing and monitoring of turbine performance by using a more flexible, cost-effective and less time-consuming device [10].

This paper presents the preliminary data obtained from an initial characterisation on the test rig of a steady-state condition of a HATT. The turbine selected to be represented on the test rig is the CMERG turbine 3.0 model [11] that has been previously validated both in CFD and experimental testing. Further turbine details will be presented herein. The main focus in this paper is on the signals output from the rotor and the generator elements of the test rig. This allows the authors to compare their power, torque and rotational frequency to the theoretical values.

This research will then be used to define the turbine dimensions and the velocities that may be simulated on the test rig. That in turn will enable the users to determine the flow conditions that may be represented from specific locations. An initial set of tests is intended to represent conditions resulting from velocities from 1.0 to 2.0 ms^{-1} similar to the ones found in the southeast part of Mexico [10]. Once the steady-state phase of the research has been performed and the test rig limitations have been found, the research will go on to represent fluid non-steady state conditions to add more complex and realistic conditions to the simulations.

This paper is organised as three main parts: the first presents a brief literature review on CM techniques and different approaches that have been developed to define CM algorithms that may prevent possible tidal turbine failures. The next section presents the approach that will be taken to enable the analysis of the three HATT drive train components, i.e. the rotor, gearbox and generator. It considers the benefits of using the drive train test rig for CM development. To do so a methodology used to obtain the numerical values based on a non-dimensional scaling will be presented. This information includes a description of the test rig and the software utilised for these simulations. Two different groups of simulations were performed: one changing the velocity values to find the highest velocity that could be represented on the test rig and the other to obtain a power curve with a velocity of 1 ms^{-1}. In the final section the findings based on this research will be discussed to effectively demonstrate that the test rig is able to represent simulations on steady-state conditions and that consequently may be able to advance to the next stage of this research.

II. Condition Monitoring of Horizontal Axis Tidal Turbines

As previously stated HATT operation and maintenance have become two of the biggest challenges to be met in establishing turbine array performance. Research is needed to find CBM techniques that can be deployed to meet these challenges. As part of this work appropriate CM approaches must be identified. Its use can be based on the principle that it should be a cost-effective and fast solution for emerging failures.

CM has been implemented on rotating electrical machines, such as generators and motors, for many years. Much of this work was aimed at high speed systems. The wind turbine industry has adopted and standardised some CM technologies for a shorter period of time. Based upon these foundations a small number of researchers have considered how to develop CM for application on HATT. This is a sensible approach, given the similarity between faults experienced on wind and tidal turbines. Even though CM techniques have been developed for HATT, their use to date has been very limited and needs further research focus.

In the context of the much lower speeds arising within HATTs work by Tavner [12] suggests that, if the speed of a rotor remains constant for a considerable amount of time, then spectral analysis can be built up and performed. Spectral analysis can be said to consider any signal processing technique that characterises the frequency content of a signal or a time series.

Some researchers have adapted this approach to make further analysis of a particular drivetrain component. Blackmore et al. [5] showed that, by using the power output signal of the turbine, they could accurately obtain estimates of blade loads. They were consequently able to monitor blades without the need for additional instrumentation. Similarly, a method called Transient Monitoring Surfaces (TMS) was engineered. This used the mean rotor torque signal and an added fluctuating component, based on fluid velocity turbulence, to represent a non-stationary condition[13]. This approach was utilised to detect rotor imbalance faults and it was found that a minimum amount of extracted data was required in order to accurately detect a fault in the system.

Finally, the use of a numerical simulation based on measured field data has been applied to generate torque and speed data that was used to predict the load and fatigue experienced by a HATT gearbox throughout its life [14]. This approach allowed the development of a prognostics model. This was used to estimate that gearboxes in HATTs will experience a shorter life compared to the ones exposed to wind load conditions.

The equipment and instrumentation needed to validate CM algorithms and techniques using a drivetrain simulator test rig has been considered [15]. Here both the properties of realistic flow conditions and the turbine rotor mechanical behaviour were incorporated. This allowed researchers to verify if the proposed technique could efficiently provide a solution for CM systems. Once the

algorithm has been validated, it could be implemented in a set-up intended for use in a flume tanks or to enable offshore simulations. Combining both accurate instrumentation and a spectral analysis tool, CM simulations can explore the benefits and downfalls of new ideas at a relatively low cost before developing the latter to a larger scale [16].

Due to the thrust loading conditions and shear stress a HATT will be subjected it is crucial to determine the main drivetrain component that CM research should primarily focus upon. Analysis of the downtime extracted from historical data relating to wind turbines and that provided by a Failure Mode and Effect Criticality Analysis (FMECA) conducted by Elasha et al. [6], proposed that the gearbox will be the most critical component of a HATT. Problems are said to occur due to the pitting and abrasive wear it would have to endure during a tidal cycle.

This has led to several different opinions whether a gearbox should be included in a HATT drivetrain or not, given its high estimated failure rate and costly components. The research carried out by Touimi et al. [17] analyses different direct-drive and indirect drive options comparing the academic and industry experiences both in tidal stream and wind devices. It was found that direct-drive options, such as the permanent magnet generators could be an attractive choice to minimise maintenance issues. These can be more expensive due to the low speed and high torque generator needed for the turbine. Given that gearbox reliability is improving and that single-stage gearboxes are considered appropriate for HATTs the decision on drive train configuration is open. This is a statement of great significance on this research to develop a CM technique based on an indirect drivetrain for a HATT simulation on a test rig.

III. METHODOLOGY

The methodology is divided in four stages: the test rig hardware used, calculation of the test rig input parameters using the theoretical HATT values based on a validated turbine, the experimental model that defines the procedure followed to characterise the turbine behaviour and finally the enactment of two test scenarios chosen to prove that the test rig can replicate the theoretical values mentioned above.

A. Test Rig Hardware

The set-up deployed to represent different HATT simulations is based on a 1/20th scale drive train test rig. This comprises two Bosch Rexroth IndraDyn MSK 050C motors (one operating as the rotor and the other one as the generator) that are coupled via a GTE 120 gearbox [10]. The test rig is shown in Fig. 1. The test rig is controlled via two IndraDrive motor drive systems. A PLC programme to emulate the aforementioned 1/20th scale HATT has been developed and embedded in the IndraDrive system. The set up used allows the rotor and generator torque to be controlled via Vector Oriented Control (VOC). In the case of the generator an additional PID control loop is undertaken, based on the feedback of an integrated encoder. Interaction with the IndraDrive devices is undertaken using the Modbus TCP/IP communication protocol, which facilitates access to the drives via PC. This connection facilitates the passing of rotor and generator commands to the IndraDrive system, whilst allowing for data collection. Fig. 2 shows a schematic diagram produced to describe the interaction between the hardware and software elements.

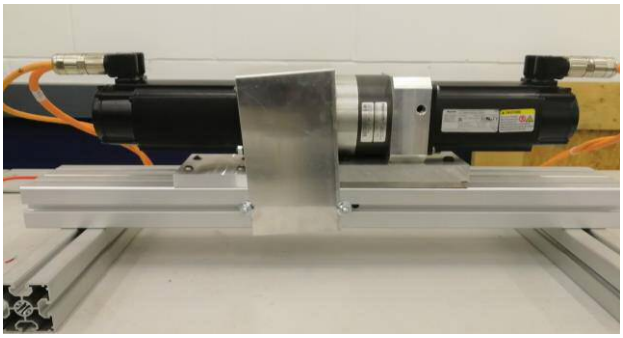

Fig. 1. The drive train test rig used to perform the simulations. A rotor is coupled to a generator via a 1:10 ratio gearbox.

The rotor and generator are Permanent Magnet Synchronous Machines (PMSMs) rated with a maximum velocity of 4700 RPM and a maximum torque of 15 Nm. The gearbox is a two-stage planetary device with a maximum input of 6500 RPM and a gear ratio of 1:10. Fig. 3 shows a graph of the speed/torque capabilities of the MSK 050Cs used in the setup. Curve 1 shows the torque speed characteristics for the voltage/current limits within the motor for a setup with three-phase 400 V controlled mains feed. This is representative of the mains setup adopted. The S1 and S3 curves show the continuous and 10-minute intermittent operation characteristics for surface cooling or natural convection setups. As the simulations are expected to be short relative to the 10 minutes operation time specified to for the S3 curve, curve 1 was used as the limiting characteristics of the test rig. The input parameters and procedure implemented on the test rig to achieve the presented simulation data will be outlined in section C.

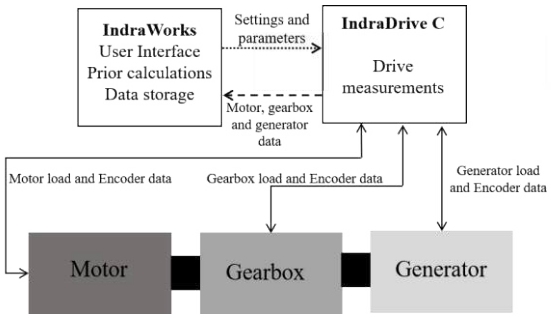

Fig. 2. Indirect-drive train test rig diagram and the distribution of functionalities across the hardware platforms.

B. Theoretical model

A theoretical model of a HATT, previously modelled and validated by CMERG [11, 18], was chosen to create the input parameters to apply to the test rig. This turbine corresponds to the CMERG Turbine 3.0 model with a turbine geometry described in Table I.

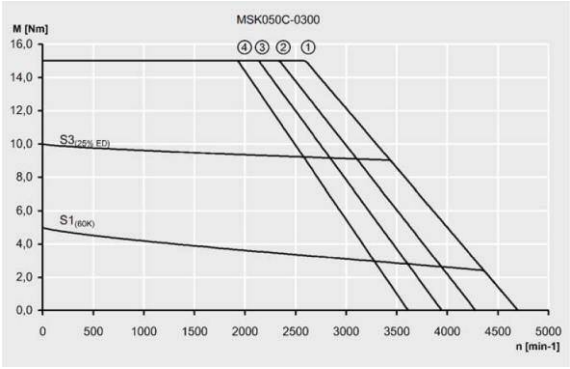

Fig. 3. Bosch Rexroth rotor/generator MSK 050Cs speed/torque characteristic.

The non-dimensional performance characteristics were determined for the turbine geometry of the CMERG Turbine 3.0 and were used as the basis of the steady-state simulations presented. Thus, torque coefficient (C_θ), power coefficient (C_p) and tip-speed ratio ( ) values from CFD results were taken to define the HATT used for the undertaken simulations.

Relying on Mason-Jones et al. [11], non-dimensional characteristics when the turbine is exposed to a uniform inlet velocity profile are taken to be independent of Reynolds number for the particular geometry utilised the development of this research. Since the research undertaken will explore the non-steady state TST simulation as a first stage, it has been considered that non-dimensional values can be used. Then, given the turbine geometry, it is possible to define a theoretical model and hence obtain the input parameters needed to simulate the turbine on the test rig.

In order to define the range of simulations achievable on the test rig a variety of turbine diameters, flow velocities and operating regions were explored. Neglecting Reynolds effects in this first instance diameters between 0.5 to 20 m were considered, with a resolution of 0.5 m, thus giving a total of 40 diameters. Velocity values ranging from 0.5 to 3 ms^{-1} with a resolution of 0.1 ms^{-1} were also considered, giving a total of 26 fluid velocities. Finally, were extrapolated from the given values from 0 to 7 with a resolution of 0.5, giving a total amount of 15 tip-speed ratios. Thus the sets of possible combinations of rotor diameter, flow velocity and tip-speed ratios were identified by combining these range of values based on equations (1) to (5). The cases selected for simulation were refined based on the results of inputting the parameter sets into equations (1) to (5).

For each one of the sets described above, to achieve the operating point or value the angular velocity ($rads^{-1}$) is given was calculated the definition of rearranged to give Eq. 1.

— (1)

The rotor power (P) and rotor Torque ( ) can be respectively calculated as follows:

TABLE I
CMERG 3.0 CFD MODEL TURBINE GEOMETRY

Turbine Specification	Value
Turbine diameter	10 m
Hub diameter	1.8 m
Blade profile	Wortmann FX 63-137
Blade twist (root to tip)	33°
Stanchion diameter	1.8 m
Nacelle diameter	2.6 m
Tower width	15 m
Tower height	15 m

– (2)

– (3)

Where V is the given fluid velocity in ms^{-1}, r is the rotor radius in m, A the rotor swept area in m^2 and the density of seawater (~1025 kg/m^3).

Based on a gear ratio of 1:10, the generator rotational velocity ( ) and the generator torque ( ) are represented as:

(4)

—— (5)

These indicate that the rotor will operate at a low speed and high torque with the generator operating at high speed and low torque.

The initial matrix of simulations with their respective calculations was reduced based on the maximum available torque from the rotor of 15 Nm, defined by the maximum torque achievable via the MSK 050Cs. Limiting the configurations to allow the highest C_p with a of 3.6, a refined set of 21 simulations were identified. Through this process a turbine of 0.5 m diameter rotor was selected with a rated fluid velocity of 1 ms^{-1}. Fig. 4 shows some of the possible variations that could be simulated on the test rig that are below the 15 Nm limit. Fig. 5 shows the C_θ- graph of the 0.5 m CMERG 3.0 turbine that was chosen for implementation on the drive train test rig.

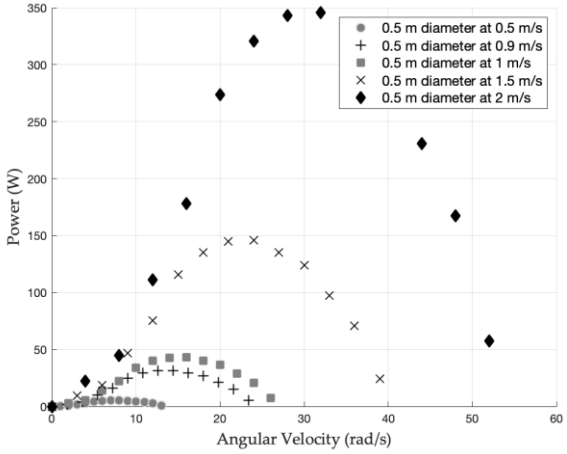

Fig. 4. Power curves with varying diameter and flow velocity.

C. *Experimental model*

As a matter of practicality, for this initial simulation the test rig was operated to behave as the modelled turbine by operating the rotor and generator in torque and speed control, respectively. Simulations of the 0.5 m diameter turbine were developed by inputting torque and speed commands based on equations 3 and 4, respectively.

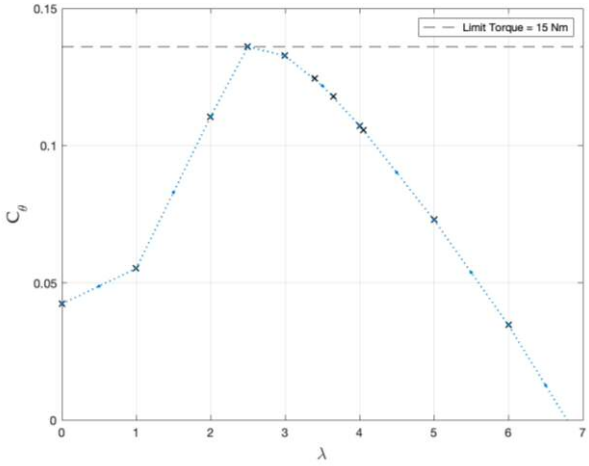

Fig. 5. Combined torque coefficient (C_θ) vs tip speed ratio ( ) with a limit torque of 15 Nm for the test rig.

For these initial simulations the proprietary Bosch Rexroth software was used to communicate the torque and speed commands to the drive systems. The software was also used to monitor rotor and generator parameters required to verify correct operation of the test rig. These parameters were recorded for each one of the cases against time (msec) and are listed in Table II along with the IndraWorks parameter number and units. The test length and sampling rate for each simulation was set to 90 secs and 33.33hz, respectively. The time length was set to allow application of the rotor torque for 60 secs, allowing for the rig to speed up and generate the required torque setting. A schematic diagram explaining the used methodology for the experimental model is shown in Fig. 6.

D. *Test scenarios*

Two test scenarios were chosen to compare the experimental model with the theoretical model. The first was a series of test at varying fluid velocities for the highest torque setting for the HATT rotor – in this case for $\lambda = 2.5$. The second test scenario was planned to represent all the values with a turbine of 0.5 m diameter and a velocity of 1 ms^{-1}. This corresponds to a $RE_{diameter}$ of 5 x 10^6 which is above the Reynolds Independent threshold for the HATT [11]. These two test scenarios had to be performed twice as the IndraWorks signals from both the rotor and the generator are recorded separately. Still, the signals can be manipulated on MATLAB and use the signal when has been manually implemented on IndraWorks. Hence, the findings of these initial characterisation simulations were analysed and compared with the theoretical model used to create the simulation parameters. This was done to check that good agreement

TABLE II
OUTPUT PARAMETERS FROM INDRAWORKS ENGINEERING

Unit number	Description
S-0-0051	Position feedback value of encoder
S-0-0084	Torque force feedback value
S-0-0040	Velocity feedback value
S-0-0381	DC bus current
S-0-0380	DC bus voltage
S-0-0382	DC bus power
P-0-0043	Torque-generating current
P-0-0044	Flux-generating current

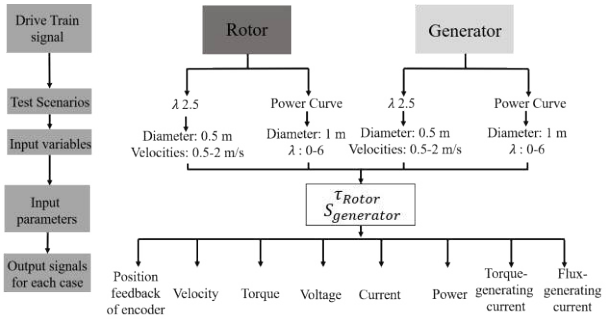

Fig. 6. Experimental model used to replicate values from theoretical model.

was found for between the simulations and theoretical turbine given system losses and motor efficiencies.

IV. RESULTS AND DISCUSSION

From the theoretical values, a selection of 16 different sets of simulations were chosen to represent all the possible highest torque inputs and hence limit the possible power curves that could be simulated on the test rig. Given a of 15 Nm limit, a of 2.5 and a 0.5 m diameter turbine, the highest velocity or cut-out speed that could be performed on the test rig is a value of 2 ms^{-1}. However, initial simulations lead to excessive heating of the motor used to recreate the turbine rotor. Whilst this was within the default temperature warnings provided by Bosch Rexroth it was considered unsuitable for both safety reasons and the likely losses in efficiencies as the motor heated excessively. Therefore, a more reserved limit was set at 11.5 Nm reducing the rate HATT speed from 2 ms^{-1} to 1.8 ms^{-1}.

On the rotor case, it was found that even though the velocity feedback value ( ) and the torque force feedback value ( ) were replicating the actual input parameters given by the theoretical model, the recorded signal from the DC bus power was higher than the expected power in each case. This is due to the induced power that the test rig uses in order to achieve the requested torque that needs to be implemented. In order to compare the rotor cases with the theoretical model, the mechanical power rather than the DC bus power of this motor was used and is given by the following equation:

(6)

is the rotational velocity feedback value recorded by the rotor encoder. Similar to the rotor case, on the generator side it was found that the velocity feedback value was replicating the actual input parameters from the theoretical values. As expected due to the rigidity of the shaft coupling used the following relationship between the rotor and generator velocities was observed:

(7)

During these simulations excessively high losses were found. The losses in the system in overcoming cogging torque from the two PMSM meant that for many simulations of lower torque settings both the rotor and generator were applying torque in the same direction. As this level of cogging torque was not expected within a HATT which would typically have only one PMSM or equivalent this effect was removed. This was done by observing the torque required to rotate the generator without the rotor applying any opposing torque. This torque value was measured for each of the rotational velocities tested and removed from the measured values as described in equations (8) and (9):

(8)

(9)

where and are the actual force feedback value and DC bus power signals measured during these initial turbine simulations and and are the force feedback value and DC bus power signals with no torque implemented by the rotor. Equations (6), (7), (8) and (9) were used both on the 2.5 and the power curve test scenarios to compare the recorded signal outputs to the theoretical model values.

E. *The fixed test scenario*

A series of test were performed at a λ-value of 2.5 for flow velocities of 0.5 to 1.8 ms^{-1}. On the rotor side, equations (1) was used to find given a -value of 2.5 and the measured output. Similarly, equation (6) was used to calculate power and compare this output with the theoretical model. Equation (9) was used to calculate power on the generator side, removing the excessively losses found within the system.

Taking the mean values of these variables from the 60 secs of the tests, a single signal for both the rotor and the generator was created. Fig. 7 shows the results obtained for the varying fluid velocity test scenario and essential shows the power developed via the simulated turbines for differing flow scenarios, given the aforementioned correction approach adopted. It can be seen that the rotor and the generator data collapses on a single exponential distribution, similar to the theoretical values. Clearly the generator data should always be less than the rotor data due to the drivetrain losses, gearbox interference and the heating losses. However, most of the generator data is either very similar to the rotor data or higher. This is likely to be due to over-correction of the losses in the system when adopting the loss correction approach described above. This notion will be studied in more detail in further work. Still, Fig. 7 shows very little variation between the theoretical values and both the rotor and generator values, representing the actual velocities and power on the test rig are as expected.

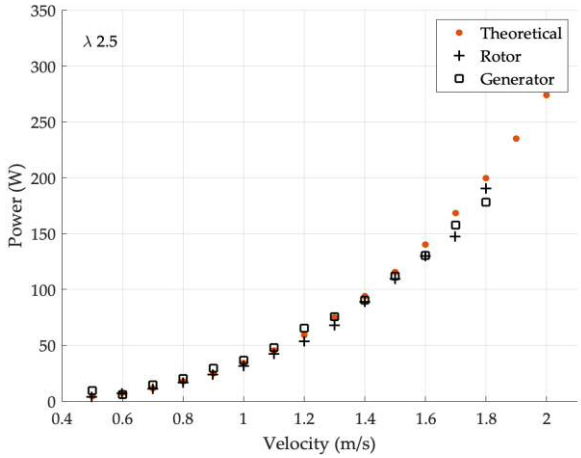

Fig. 7. Combined Power output and velocities from rotor and generator compared to the theoretical model.

F. *Fixed Power Curve test scenario*

In order to represent all -value with a turbine of 0.5 m diameter and a velocity of 1 ms^{-1}, equation (3) was used to get C_p from the output power for both the generator and the rotor to compare the theoretical model power curve to the ones generated on the test rig. Fig.8 shows the results of the fixed flow velocity simulations undertaken. Fig. 8 demonstrates how most of the points fall on a single curve with some losses through the points. There are some cases were the generator side still delivers more power compared to the rotor side, but as explained before, is being calculated using equation (9), that uses the aforementioned correction formula which have to be altered in future simulations.

Despite this problem, the rotor and the generator develop the same curve characteristics as the ones expected base on the theoretical model. The highest C_p that could be reached by the test rig with a diameter of 0.5 m is 0.39 relying on the rotor and generator data, compared to a 0.43 by the theoretical model. There was only one point through the curve given by the generator at 6 that decreased from the actual theoretical value by 19.14%. This finding was unexpected as the torque/speed characteristic of the motor presented in Fig.3 shows that the motor should operate as expected. The excessive losses in this case maybe down to motor heating which would lead to higher electrical losses in the system.

Fig. 9 demonstrates the torque implemented on both the rotor and the generator compared to the rotor angular velocity, . This graph represents the given values from the test rig are as expected. The generator signal decreases its efficiency from the rotor signal but both fall onto the same curve characteristic from the theoretical

values. There are some small drops in torque at angular velocities of 0 and 24 rads^{-1}. Fig. 9 shows that the theoretical and experimental model collapses onto the same curve as that produced using a steady-state CFD modelling validated via flume experiments.

This correlation between theoretical and experimental data indicates the potential and flexibility for using the test rig for future research. This will explore unsteady state conditions and be used to define an approach for an initial characterisation based on the selected turbine geometry. Moreover, it will allow researchers to explore the concept of using speed and torque control to analyse their electric signals for turbine monitoring. However, it should be noted that this analysis will be initially limited to the selected turbine geometry. As such further complex and realistic conditions should be added to the experimental model, i.e. turbulence intensity on the flow characterisation and a parametric model changing the tip-speed ratio on a HATT turbine. Nevertheless, the test rig will allow users to simulate different turbine geometries, velocity and tip-speed ratio input. This research will then move on to focus on the unsteady state conditions to be added on the test rig in the future.

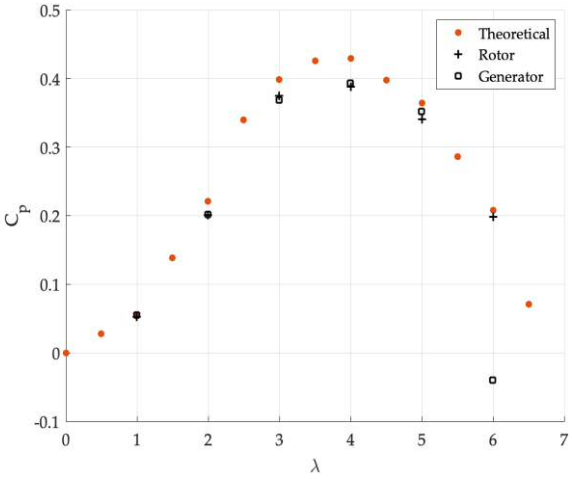

Fig. 8. Power Curve with from rotor and generator compared to the theoretical model of a 0.5 m diameter turbine at 1 ms^{-1}.

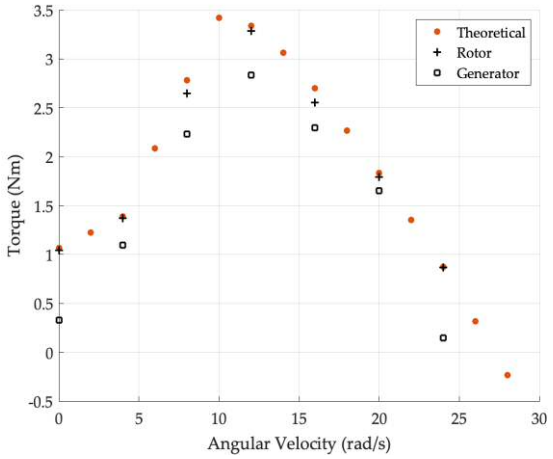

Fig. 9. Combined Torque with Angular velocity from rotor and generator compared to the theoretical model of a 0.5 m diameter turbine at 1 ms^{-1}.

V. CONCLUSION

It has been demonstrated that an initial characterisation of a drive train test rig simulating a particular HATT design operating in steady flow conditions can be achieved. Based on a theoretical model to calculate the rotor torque and the generator rotational frequency, these values can be implemented as input parameters to replicate the conditions of the theoretical model and model a power curve up of a diameter of 0.5 m. It has been shown that a velocity of 1.8 ms^{-1} can be modelled on a test rig with a 0.5 m diameter turbine given a 11.5 Nm limit rotor torque. These two test scenarios allow the research to enable the use of a test rig for further condition monitoring research. Further work is required to understand the losses in the system to more accurately represent the drive train dynamics of a 0.5 m diameter HATT.

REFERENCES

[1] D. Magagna and A. Uihlein, "Ocean energy development in Europe: Current status and future perspectives," *International Journal of Marine Energy*, vol. 11, pp. 84-104, 2015. DOI: 10.1016/j.ijome.2015.05.001 [Online].

[2] DECC. (2008). *Tidal-current Energy Device Development and Evaluation Protocol*. Aug. 2008. [Online] Available: https://webarchive.nationalarchives.gov.uk/+/http:/www.berr.gov.uk/files/file48401.pdf

[3] D. Coles, C. Greenwood, A. Vogler, T. Walsh, and D. Taaffe, "Assessment of the turbulent flow upstream of the Meygen Phase 1A tidal stream turbines," presented at the 4th *Asian Wave and Tidal Energy Conference,Taipei*, 2018.

[4] A. Davies, *Handbook of condition monitoring : techniques and methodology*. London : Chapman & Hall, 1997.

[5] T. Blackmore, L. E. Myers, and A. S. Bahaj, "Effects of turbulence on tidal turbines: Implications to performance, blade loads, and condition monitoring," *International Journal of Marine Energy*, vol. 14, pp. 2016. DOI: 10.1016/j.ijome.2016.04.017, [Online].

[6] F. Elasha, D. Mba, and J. A. Teixeira, "Condition monitoring philosophy for tidal turbines," *International Journal of Performability Engineering*, vol. 10, no. 5, pp. 521-534, 2014 [Online].

[7] M. Allmark, R. Grosvenor, and P. Prickett, "An approach to the characterisation of the performance of a tidal stream turbine," *Renewable Energy*, Article vol. 111, pp. 849-860, 2017. DOI: 10.1016/j.renene.2017.05.010, [Online].

[8] R. I. Grosvenor, P. W. Prickett, and H. Jianhao, "An assessment of structure-based sensors in the condition monitoring of tidal stream turbines," in *2017 Twelfth International Conference on Ecological Vehicles and Renewable Energies (EVER)*, 2017, pp. 1-11.

[9] M. Allmark, "CM and Fault Diagnosis of Tidal Stream Turbines Subjected to Rotor Imbalance Faults.," Ph.D. dissertation, ENGIN, Cardiff University, Cardiff University, 2016.

[10] E. Rojo-Zazueta, I. Mariño-Tapia, R. Silva-Casarín, M. Allmark, P. Prickett, and R. Grosvenor, "Defining a Marine Turbine Condition-Based Maintenance and Management Strategy for Low Velocities in Mexico," presented at the 4th *Asian Wave and Tidal Energy Conference, Taipei*, 2018.

[11] A. Mason-Jones *et al.*, "Non-dimensional scaling of tidal stream turbines," *Energy*, vol. 44, no. 1, pp. 820-829, 2012. DOI: 10.1016/j.energy.2012.05.010, [Online].

[12] P. Tavner, "Review of condition monitoring of rotating electrical machines," *IET Electric Power Applications*, vol. 2,

no. 4, pp. 215-247, 2008. DOI: 10.1049/iet-epa:20070280, [Online].

[13] M. Allmark, P. Prickett, and R. Grosvenor, "Detection of Tidal Stream Turbine Rotor Imbalance Faults for Turbulent Flow Conditions and Optimal Tip Speed Ratio Control," presented at the *12th European Wave and Tidal Energy Conference, Cork,* 2017.

[14] F. Elasha, D. Mba, J. A. Teixeira, and B. Cranfield, "Failure Prediction of Tidal Turbines Gearboxes," *eMaintenance,* p. 49, 2014. DOI: 10.13140/RG.2.1.1080.4563, [Online].

[15] W. Yang, P. J. Tavner, C. J. Crabtree, and M. Wilkinson, "Research on a simple, cheap but globally effective condition monitoring technique for wind turbines," in *2008 18th International Conference on Electrical Machines*, 2008, pp. 1-5.

[16] D. A. Doman, R. E. Murray, M. J. Pegg, K. Gracie, C. M. Johnstone, and T. Nevalainen, "Tow-tank testing of a 1/20th scale horizontal axis tidal turbine with uncertainty analysis," *International Journal of Marine Energy,* vol. 11, pp. 105-119, 2015. DOI: 10.1016/j.ijome.2015.06.003, [Online].

[17] K. Touimi, M. Benbouzid, and P. Tavner, "Tidal stream turbines: With or without a Gearbox?," *Ocean Engineering,* vol. 170, pp. 74-88, 2018. DOI: 10.1016/j.oceaneng.2018.10.013, [Online].

[18] C. H. Frost, P. S. Evans, C. E. Morris, D. M. O'Doherty, and T. O'Doherty, "Flow Misalignment and Tidal Stream Turbines", presented at the *11th European Wave and Tidal Energy Conference, Nantes,* 2015.